RANS Turbulence Modeling for Supercritical Carbon Dioxide Flows

Timothy P. Grunloh*, Luke Calian
Illinois Rocstar LLC
108 Hessel Blvd
Champaign, IL 61820
www.illinoisrocstar.com
*tpgrunloh@illinoisrocstar.com

Dr. Timothy P. Grunloh is a research scientist at Illinois Rocstar, LLC. Dr. Grunloh received his Ph.D. in Nuclear Engineering and Radiological Sciences from the University of Michigan in 2016. During his Ph.D. work he developed a multi-scale fluid coupling infrastructure to link high fidelity computational fluid dynamics (CFD) software to low fidelity systems analysis software for the simulation of nuclear power plants under transient conditions. His experience includes developing scientific software as well as leveraging high performance computing resources to perform CFD analyses of a wide variety of flows, including both compressible and incompressible regimes. In particular, he has a great deal of experience applying Reynolds Averaged Navier-Stokes (RANS) turbulence models, especially nonlinear eddy viscosity models, to complex flows.

1 Introduction

As energy appetites around the world continue to grow, hydrocarbon fuels will contribute substantially to the energy portfolio for the foreseeable future. At the same time, concerns of climate change are increasingly motivating the development of energy sources that contribute less to atmospheric carbon levels, motivating use of carbon capture technologies. Oxy-fuel fired power plants offer substantially lower carbon capture costs than traditional flue gas scrubbing[1]. Recent interest in this combustion type has been focused on CO_2 rich environments[2] such as supercritical CO_2 (sCO_2) power cycles, which additionally allow for improved thermodynamic efficiency and more compact facilities. sCO_2 power cycles have been found to provide 99% carbon capture at a 21% reduction in cost compared to supercritical steam cycles [3]. Using supercritical carbon dioxide (sCO_2) as a working fluid in power cycles also enables operation at higher thermodynamic efficiency. Indeed, according to [4], sCO_2 cycles can improve upon the efficiency of traditional steam Rankine cycles by 5%.

As sCO_2 cycles are designed, evaluated, and deployed, modeling and simulation (M&S) activities are carried out alongside experimental studies to support safe, economically optimized design and operation. Among existing computational approaches to turbulence, only Direct Numerical Simulation (DNS) methods fully resolve turbulent effects. Unfortunately, DNS methods are prohibitively expensive for most cases. Large Eddy Simulation (LES), which resolves some scales of turbulence, is too expensive and time consuming for applications including design and optimization, which require from 10 to 10^6 (or more) simulations. Despite this, LES is ideal in specific situations when intricate flow details are required, such as resolving thermal striping phenomena. Reynolds-Averaged Navier-Stokes (RANS) turbulence models are ideal for design and optimization applications that either require large numbers of simulations or do not require resolution of very fine scales of the flow field. RANS models are not universally applicable, therefore we have developed models in *OpenFOAM* specifically for supercritical flows.

Supercritical fluid modeling is required for a number of processes in power plants. The United States Department of Energy (DOE) has identified several components of direct-fired cycles that are specifically in need of additional research and development. Among the components identified are pressurized oxy-combustion and sub-critical CO_2 pumping and compression [5]. Combustion within the working fluid generates strong temperature and density gradients, leading to a number of phenomena including strongly enhanced turbulent mixing and potentially strong buoyancy effects. Control of turbomachinery is difficult near the critical point, which necessitates precise and accurate models for pump design. Furthermore, thermal transport in heat exchangers leads to strong near-wall temperature gradients and buoyancy effects. The models in this paper were formulated to specifically address the simulation of buoyant supercritical flows. Development of the models involved combining the shear stress transport models with an advanced formulation of the turbulence-temperature correlation, or buoyancy production term, then explicitly tuning coefficients to sCO_2 flows.

The work in this paper employs an Algebraic Flux Model (AFM) formulation for the turbulence-temperature correlation. Because this approach requires the solution of additional transport equations alongside the standard two equation turbulence models, the generated models are collectively referred to as "four equation models." To the knowledge of the authors, the formulation of the additional transport equations used here is novel. Relevant publications typically use a k_t-ε_t ($k_t = \overline{T'^2}$ and the t subscript refers to temperature T) formulation analogous to the k-ε turbulence model [6, 7, 8], while we employ a k_t-ω_t formulation analogous to the k-ω turbulence model. This formulation was chosen to leverage the superior near-wall performance of the k-ω model. Models were tested in two regimes based on flow rates. We have found that models developed on heated tube experiments with low flow rates did not perform well when applied to higher flow rates, and vice versa. In general, we established that the algebraic flux model was critical for low flow rate applications and also particularly important for more moderate flow cases.

2 Modeling Approach

This section describes the modeling framework used in the presented work. The thermal properties of the supercritical fluids were found to play a very significant role, and the approach to including the temperature dependence for important properties such as density, specific heat, and viscosity is discussed in Section 2.1. The motivation behind the selection of AFM for the buoyancy production term is discussed in Section 2.2 and the specific formulation used is detailed in Section 2.3.

2.1 Equation of State

A key characteristic of supercritical fluid is the variation of thermodynamic variables with temperature. The National Institutive of Standards and Technology (NIST) freely provides accurate, tabulated values for these properties[1]. The version of *OpenFOAM* used for this work (v4.1) did not natively support using lookup tables for Equation of State (EOS). Fortunately, a member of the large *OpenFOAM* user community has provided this functionality[2], which was incorporated into the software used in this work. For the cases studied in this work, we assumed a pseudo-isobaric EOS. Specifically, we evaluated temperature-dependent properties at a single pressure for each simulation. For sCO_2, properties were evaluated at pressures of 8.194 MPa and 8.419 MPa. The *OpenFOAM* formulation uses density (ρ), enthalpy (h), isobaric specific heat (c_p), isobaric specifc heat minus isochoric specific heat ($c_p - c_v$), dynamic viscosity (μ), thermal conductivity (κ), and thermal expansion coefficient (β). These data are taken from the NIST resource and processed via Python into lookup tables suitable for *OpenFOAM*. We found that using a single representative constant for properties was insufficient. We briefly studied fitting thermodynamic properties to polynomial functions, but quickly found this unsuitable to capture supercritical flow physics.

2.2 Motivation for Algebraic Flux Model

Due to the sensitive variation of thermophysical properties with temperature, supercritical fluids exhibit complex behavior. For example, consider flow of supercritical fluid through a heated channel in a gravitational field, a problem well supported by a wealth of published data [9]. For upward flow, the buoyancy production term plays a key role in heat transfer deterioration arising from laminarization. Bae et al. [10] showed through DNS that any increase in wall temperature following heat transfer deterioration is limited by axial profile flattening with accompanying decreased shear stress production. This can lead to a change in sign of buoyant forces, which can dominate shear stress effects in the boundary layer. Bae et al. also found that, in downward flows, the buoyancy

[1] http://webbook.nist.gov/cgi/cbook.cgi?ID=C124389
[2] https://github.com/Ldenies/tabulatedProperties

effect increases the turbulence level, which enhances heat transfer. Standard models have been found generally unable of simulating these phenomena [11]. A more sophisticated algebraic flux model approach has been investigated by a number of authors over the past several decades [7, 12, 13, 14, 15, 16]. In general, the simulation of highly buoyant flows, such as those expected with supercritical fluids, is a particularly active field of inquiry [17, 18, 19].

One such study, performed by Kim and Kim[20], is summarized in Fig. 1. This figure shows experimentally measured wall temperatures along the heated section of upward sCO_2 flow for three cases with "low" flow rates. The cases are differentiated modestly in terms of system pressure, flow rate, and applied heat flux. As is clear from the figure, the qualitative and quantitative behavior of the heat transfer can be exceedingly sensitive to the flow conditions. Case c featured the lowest flow rate and highest heat flux of the set. Consequently, these data exhibit interesting behavior in the form of a striking temperature peak within the heated section, a phenomenon also observed in the DNS simulations of Bae et al. [10].

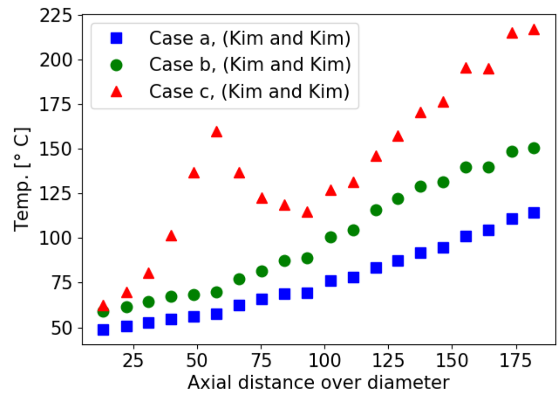

Figure 1: Data collected by Kim and Kim[20] of sCO_2 flow through heated channel.

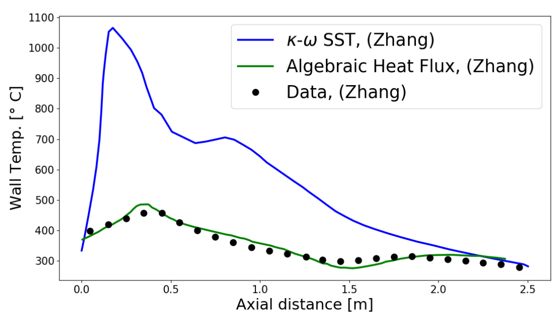

Figure 2: Summary of analysis by Zhang[7] showing simulation of supercritical water flow through heated channel.

Zhang et al. [7] performed compelling analyses of the utility of using AFM for buoyancy production of turbulence. The authors performed experimental measurements of wall temperatures along heated channels of supercritical water. They additionally performed simulations of the experiment with the intention of assessing various turbulence models' ability to capture physics relevant to supercritical flows.

Consider Fig. 2 as a summary of their results. In this case, the SST model strongly overpredicted wall temperatures. However, the Zhang formulation of AFM (using k-ε turbulence and k_t-ε_t AFM) quite accurately captured the experimental data qualitatively and quantitatively.

2.3 Illinois Rocstar Formulation

The specific model used in this paper uses Shear Stress Transport (SST) for Reynolds stress closure and a k_t-ω_t AFM formulation for the buoyancy production term. The SST model combines the k-ω and k-ε turbulence models such that the models behave like k-ω in the boundary layer and k-ε in the interior, free shear flow region [21]. Over recent years, this model has gained traction and is a major model supported by many CFD packages. The SST model implemented in *OpenFOAM* was based on the description provided by Menter and Esch [22] with updated coefficients [23] and an optional term for rough walls adapted from Hellsten [24].

While the majority of AFM implementations found in the literature use a k_t-ε_t formulation, we employed a k_t-ω_t formulation. We hypothesized that the superior near wall behavior of k-ω would translate to improved behavior of the entire four-equation model. Existing k-ε-k_t-ε_t models employ a number of damping functions to improve near wall model. By using fewer function entities, the applicability of this model is likely to be wider. The k_t-ω_t AFMs were implemented by adding the transport equations of Eq. 1 and Eq. 2 to existing turbulence models:

$$\frac{\partial \rho\omega_t}{\partial t} + \overline{u}\cdot\nabla\left(\rho\omega_t\right) - \nabla\cdot\left[\rho\left(\alpha_{\omega_t}\nu_T + \nu\right)\nabla\omega_t\right] = \rho\gamma_t G_t\frac{\omega_t}{k_t} - \frac{2}{3}\rho\gamma_t\nabla\cdot\overline{u}\omega_t - \beta_t\rho\omega_t^2, \tag{1}$$

$$\frac{\partial \rho k_t}{\partial t} + \overline{u}\cdot\nabla\left(\rho k_t\right) - \nabla\cdot\left[\rho\left(\alpha_{k_t}\nu_T + \nu\right)\nabla\omega_t\right] = \rho G_t - \frac{2}{3}\rho\nabla\cdot\overline{u}\omega_t - C_{\mu_t}\rho\omega_t k_t, \tag{2}$$

where G_t is given by:

$$G_t = \overline{u_i'T'}\frac{\partial\overline{T}}{\partial x_i}, \tag{3}$$

and the turbulence anisotropy tensor is given by

$$a_{ij} = \frac{\overline{u_i'u_j'}}{k} - \frac{2}{3}\delta_{ij}. \tag{4}$$

The addition of these transport equations allows for the calculation of $\overline{T'^2} = k_t$ which, in turn, allows for the calculation of the $\overline{u_j'T'}$ correlation as defined by Eq. 5:

$$\overline{u_j'T'} = -C_t\tau\left[C_{t1}\overline{u_i'u_j'}\frac{\partial\overline{T}}{\partial x_i} + \left(1-C_{t2}\right)\overline{u_i'T'}\frac{\partial\overline{u}_j}{\partial x_i} + \left(1-C_{t3}\right)\beta g_j\overline{T'^2}\right] + c_{t1}'a_{ij}\overline{u_i'T'}, \tag{5}$$

where β is given by:

$$\beta = -\frac{1}{\rho}\frac{\partial\rho}{\partial\overline{T}}. \tag{6}$$

Once calculated, $\overline{u_j'T'}$ actually affects the flow through source terms to the k and ω transport equations. Some published values for the AFM coefficients are given in Table 1.

Table 1: Selected AFM coefficients from literature.

Model	C_t	C_{t1}	C_{t2}	C_{t3}	c_{t1}'
Kenjereš [16]	0.15	0.6	0.4	0.4	1.5
Zhang [7]	0.66	1	0.33	0.33	0

3 Results

In Section 2, the turbulence models used and developed for the efforts described in this paper were described theoretically. In this section, we tailor the models to realistic simulations and compare the results to previously published experimental data. Section 3.1 discusses the approach taken to develop the models, with the produced models presented in Section 3.2. Broadly speaking, the approach uses experimental data from sCO_2 flows to inform model formulations. By developing models from sCO_2 data, we seek to create RANS models that are uniquely suited to capture the complex physical phenomena characteristics of supercritical fluids.

3.1 Coefficient Optimization

Turbulence models generally contain a number of semi-empirical or empirical coefficients. Common models such as k-ε or k-ω are often considered alongside standard sets of coefficients, which are generated by comparing model results against sets of canonical flow problems. Because this set of problems is finite, the traditionally quoted sets of model coefficients cannot be applied to every possible flow with an expectation of high quality results. Therefore, a key aspect of developing turbulence models specific to sCO_2 flows involves calculating optimized sets of model coefficients.

Optimization of coefficients based on experimental data was carried out in Python using the *SciPy* package. A wrapper was written to allow the "least_squares"[3] function to run *OpenFOAM* with a set of input parameters. A function within the Python wrapper wrote the input parameters into the "turbulenceProperties" file that *OpenFOAM* uses to select the turbulence model and to change coefficients.

As discussed by Duffey and Pioro [9], a wide variety of studies on supercritical flow through heated channels have been reported in the literature over the past few decades. The model development effort discussed here was guided by the objective of simulating the experiment performed by Kim and Kim [20], wherein data is presented from a number of experimental cases. This particular study was utilized because the experiments were straightforward to explore and the reported results included complex phenomena. We chose two cases from Kim and Kim's study (key parameters are listed in Table 2, both for upward flows) to guide the turbulence modeling work. The "lowFlow"case is characterized by a low flow rate such that buoyancy effects are expected to play a substantial role. A more moderate flow rate case is referred to as "modFlow". Buoyant effects are expected to play a less critical role in this scenario. Considering both cases enables us to analyze multiple physical mechanisms and to chart a path forward for developing RANS models capable of simulating wide ranges of supercritical fluid flows.

Table 2: Chosen test case parameters from Kim and Kim [20].

Case	Inlet Velocity [m/s]	Pressure [MPa]	Heat Flux [kW/m^2]	Fluid
lowFlow	0.31	8.194	82.6	CO_2
modFlow	0.67	8.419	103.1	CO_2

The "lowFlow" case (Case c in Fig. 1) exhibits a local temperature peak a short distance downstream of the inlet of the heated section. This feature is a result of "heat transfer deterioration", a phenomenon discussed by several authors [6, 7]. While many factors contribute to heat transfer deterioration, it is a key factor in buoyant supercritical flows and test cases were specifically chosen to include it.

[3] https://docs.scipy.org/doc/scipy-0.19.1/reference/generated/scipy.optimize.least_squares.html

3.2 Model Development

A "coarse" mesh was used for a wall-modeled simulation. This mesh features 3 prism layers near the edge as the turbulent boundary layer is primarily modeled. The coarse mesh is 395,600 cells in total with an average of ≈ 7.12 faces per cell. This total includes 154,800 hexahedra and 240,800 polyhedra.

The models we created are further discussed in Section 3.2.1, in the context of the Kim and Kim data used to generate them. In Section 3.2.2, the models are used to compute the Kim and Kim scenarios that they were not developed from (i.e., a model tuned from "lowFlow" data is used to simulate the "modFlow" case). We refer to this as "testing" rather than validation because the data are part of the same experiment and are subject to common cause faults. Lastly, an additional model referred to as AFMSST.lfmf.1 was developed using both sets of data.

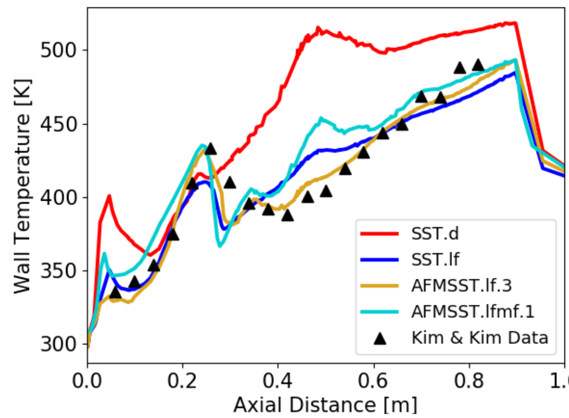

Figure 3: Comparison of SST-based models from the "lowFlow" case.

In the sections to follow, we present results in terms of wall temperature along a heated section of upward axial flow. Note that all experimental data were captured from thermocouple measurements. An axial distance of 0 represents the entrance of the heated section and larger axial distances represent higher elevations.

3.2.1 Model Tuning

Fig. 3 shows the results of model coefficient fitting for sCO_2 turbulence models based on the SST model. With the exception of the default SST (SST.d) curve, all plots were calculated with coefficients calculated from fitting the experimental data from Kim and Kim [20]. The specific data used from the "lowFlow" case of Table 2 are also plotted in Fig. 3. The SST.d poorly represents the data, both qualitatively and quantitatively.

The SST model with optimized coefficients (SST.lf) is significantly better at representing the curve. The left edge of the internal temperature peak is particularly well predicted while the right edge is less well represented. The remainder of the curve provides a reasonable, qualitative reproduction of the overall trend of the data. We added the algebraic flux model to the standard SST model and optimized to generate several sets of coefficients.

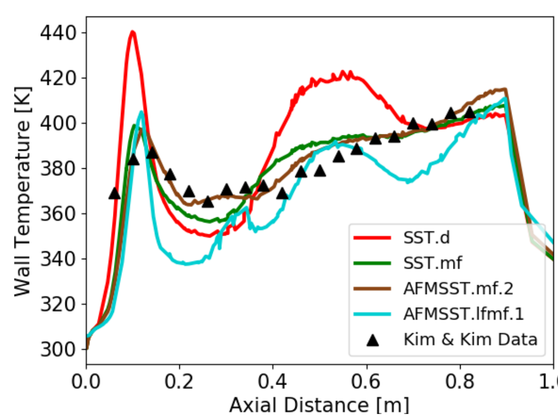

Figure 4: Comparison of SST-based models for "modFlow" case.

The AFMSST.lf.3 curve shows the best representation of the experimental data: the left edge of the internal temperature peak is well resolved and the local maximum is also quite well reproduced. The right edge of the internal peak is somewhat poorly predicted once again. The remainder of the experimental data are well represented, both qualitatively and quantitatively. The AFMSST.lfmf.1 model, tuned from both sets of data, matches the internal temperature peak very well. However, this model shows another peak around the axial distance of 0.5 that is likely an artifact from the “modFlow” case.

All coefficients are given in Table 3, which shows the coefficients for the k_t and ω_t transport equations and Table 4, which shows the coefficients from the SST portion of the AFM model (i.e., k and ω transport equations). It should be noted that these results do not provide information about the predictive capability of the models since they are being compared to data to which they are fit. However, this figure does provide information about which models are able to actually resolve the physics of the model. These results suggest that the addition of AFM to the SST model improves our ability to resolve heated, supercritical fluid behaviors.

Table 3: AFM coefficients for RANS models developed for sCO_2 flows.

Model	C_t	C_{t1}	C_{t2}	C_{t3}	c'_{t1}	β_c	β_t	$C_{\mu t}$	γ_t	α_{k_t}	α_{ω_t}
AFMSST.lf.3	1.0	0.95	1.31	1.58	2.03	1.0	0.072	.09	0.52	0.5	0.5
AFMSST.mf.2	1.0	0.64	1.88	1.44	1.24	1.0	0.072	.09	0.52	0.5	0.5
AFMSST.lfmf.1	1.0	1.12	1.87	1.46	0.83	1.0	0.072	0.09	0.52	0.56	0.6

These coefficients were used in conjunction with the corresponding coefficients in Table 4

Table 4: SST Coefficients coefficients for RANS models developed for sCO_2 flows.

Model	α_{k1}	α_{k2}	$\alpha_{\omega 1}$	$\alpha_{\omega 2}$	γ_1	γ_2	β_1	β_2	a_1	b_1	c_1
SST.d	0.85	1.0	0.5	0.856	γ_d	0.44	0.075	0.0828	0.31	1.0	10
SST.lf	0.43	1.47	0.72	0.16	0.82	1.11	0.11	0.11	0.32	0.84	43
SST.mf	0.677	1.95	0.61	0.877	0.71	0.62	0.088	0.104	0.754	1.25	29
AFMSST.lf.3	0.0034	1.4	0.59	0.012	0.507	0.84	0.075	0.0828	0.31	1.0	10
AFMSST.mf.2	0.0827	1.072	0.325	0.25	0.676	0.715	0.075	0.0828	0.31	1.0	10
AFMSST.lfmf.1	0.21	0.26	0.96	0.056	0.25	0.85	0.075	0.0828	0.71	0.91	9.53

SST.d = SST model with default coefficients
SST.lf = SST model with coefficient tuned to “lowFlow” case
SST.mf = SST model with coefficient tuned to “modFlow” case
$\gamma_d = 0.555556$

Fig. 4 shows the results of fitting exercise based on the “modFlow” case from Table 2. Once again, the standard SST model (SST.d) does not well represent the wall temperature along the heated section and exhibits strongly exaggerated features. An optimized SST model (SST.mf) is significantly better at representing the target data. The AFMSST.mf.2 model with AFM transport equations was also tuned to the “modFlow” data and was able to represent the data moderately better than the optimized SST model.

3.2.2 Model Testing and Discussion

Fig. 5 shows the results of testing “modFlow” tuned cases on the “lowFlow” scenario. All models line up well with the left edge of local peaking. However, only AFMSST.lfmf.1 is able to capture the lower temperature after the peak. The default SST model (SST.d) and models tuned to only the “modFlow” data fail to represent key physics of the supercritical fluid. Comparing the AFM coefficients (Table 3) shows that the primary difference between AFMSST.mf.2 and AFMSST.lfmf.1 are the C_{t1} and SST transport equation coefficients, highlighting the importance of the temperature gradient and turbulent mixing. The c'_{t1} coefficient is also somewhat different, but SST is a linear model and the turbulence anisotropy tensor will not contribute. This term was included for completeness and the value produced is likely a fitting artifact.

Fig. 6 shows the results of testing "lowFlow" tuned cases on the "modFlow" scenario. The AFMSST.lf.3 model behaves smoothly but significantly underpredicts the wall temperature and misses all qualitative features of the data. The SST.lf model approximately captures the small peak towards the left of the plot but underpredicts the wall temperature throughout the remainder of the heated section. In this case, the best performing model is the SST model with standard coefficients. SST.d qualitatively captures the peak near the inlet of the heated section and captures wall temperature "on average," in that the calculated temperature remains near the measured temperature.

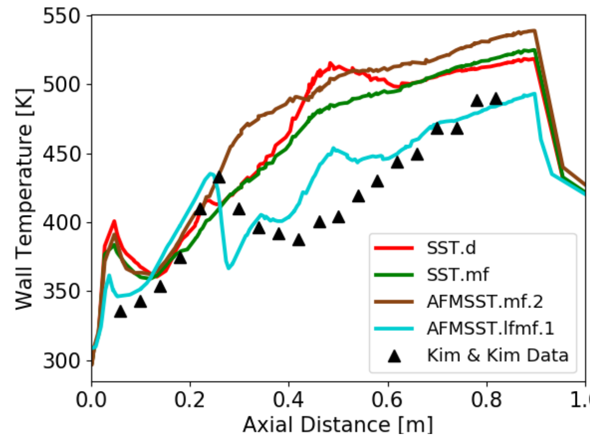

Figure 5: Testing of SST-based models on "lowFlow" case.

The results suggest that the models tuned to one data set perform best within a flow rate regime. For example, the AFMSST.lf.3 model represents the "lowFlow" data especially well, shown in Fig. 3, but essentially fails to capture the temperature profile of the "modFlow" case, shown in Fig. 6. The same trend was provided for the cases tuned to the "modFlow" data. These observations motivated the creation of the AFMSST.lfmf.1 model, which was informed by both sets of data. While this model does not perfectly match either set of data, it outperforms the standard SST model as well as the other fitted models.

The models created during this work were subject to several iterations of the fitting procedure, as indicated by the number at the end of each model name. Continued iteration on the lfmf model in the form of adjustments made to the starting set of coefficients or fitting subsets of coefficients separately is likely to improve the performance of the model. At this point, the predictive capacity of these models is uncertain. Validation through comparisons to experimental data will be subject to substantial future efforts. However, preliminary testing has shown that a version of the AFMSST.mf.X series of models exhibits predictive properties for supercritical fluids with moderate flow rates. These results will be published in an upcoming paper. The continued development and assessment of these models is the subject of ongoing and future work.

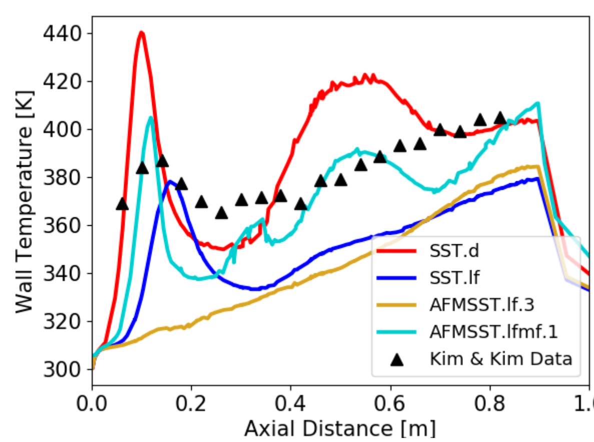

Figure 6: Testing of SST-based models on "modFlow" case.

As discussed in detail in Sections 2 and 3, this work uses pre-published experimental data from the scientific literature which primarily consists of forced flow through heated tubes. The additional physics added to the RANS models through the k_t-ω_t transport equations has demonstrated the ability to simulate thermal phenomena of supercritical fluids, such as heat transfer deterioration. At this point, the models have only been tested on upward flow. With downward flow, heat transfer enhancement occurs because the buoyant effects increase turbulent mixing. The applicability of the presented models to such scenarios is a question of future inquiry. The targeted application of the work in this paper is power cycles using supercritical working fluids in which we foresee three primary sub-applications: (1) heat exchangers, (2) turbomachinery, and (3) combustors.

4 Conclusions and Future Work

We designed, implemented, and optimized a framework for the production of RANS turbulence models based on existing experimental data published in the scientific literature. This framework produced several novel four-equation k_t-ω_t turbulence models based on SST RANS models along with the algebraic flux model for the buoyancy production term. We developed the models iteratively by tuning coefficients to published data from experimental programs conducted on heated tubes with forced sCO_2 flow. Optimized models with AFM transport equations were shown better able to represent complex phenomena such as heat transfer deterioration than standard RANS models without AFM. The predictive capacity of these models is presently uncertain. Validation will be the subject of substantial future efforts. However, preliminary testing has shown that a version of the AFMSST.mf.X series of models exhibits predictive properties for supercritical fluids with moderate flow rates, to be published in an upcoming paper.

Our ongoing work will focus on expanding the data set to which the models are tuned with hopes of widening the range of applicability. For example, optimizing coefficient sets with both "lowFlow" and "modFlow" data is hoped to produce a predictive model with less restriction on system flow rate. Further, we are interested in developing improved wall treatment formulations for future models. The treatment used here was based on existing formulations for the standard k and ω fields. More advanced wall functions may be constructed to include buoyant effects that can potentially increase the fidelity of these models [25, 26, 27] with sensitivity to anisotropic turbulence and streamline curvature added through nonlinear constitutive models. We anticipate that adding these into supercritical flow models will improve capabilities for highly complex flows such as those found in combustors or turbomachinery.

The isobaric assumption employed here for material properties is unlikely to hold in combustors. Therefore, these models will be integrated with more advanced equations of state to broaden the applications of the model. See Section 4.1.1 for more details. The data we used to optimize model coefficients were composed only of wall temperatures. In future work, we intend to leverage more detailed data as it becomes available to optimize specific correlations alongside system-scale quantities.

4.1 Consideration for Complex Applications

The models we have presented in this paper were targeted toward flows wherein buoyancy was a key phenomenon. This technology can be directly applied to certain types of heat exchangers which are well-described by pipe flow. Buoyancy may also play a role in compressors under certain conditions when large pressure differences lead to large density differences. However, buoyancy effects will not be dominant in many scenarios relevant to sCO_2 power cycles, such as those characterized by very high flow rates. The work documented in this paper was carried out with the intention of future extensions to power cycle applications with specific interest in turbomachinery and combustor simulation.

4.1.1 Equations of State

For the work in this paper, we used an isobaric equation of state. This assumption is likely to break down for many turbomachinery and combustor applications. Therefore, incorporation of more sophisticated equations of state will be a crucial step moving forward. Manikantachari et al. identified the Soave-Redlich-Kwong EOS [28] as applicable to direct-fired sCO_2 combustor applications [29], while Ghosh compared this EOS to the Peng-Robinson model [30]. Future incorporation of these EOS's in our *OpenFOAM* sCO_2 models will be a straightforward affair.

4.1.2 Combustors

We will leverage the experience gained developing new turbulence models to extend the sCO_2 models to combustion environments. This effort will involve coupling advanced turbulence-species concentration correlations interaction with turbulent mixing from sCO_2 focused models and incorporation of advanced equations of state (EOS). To illustrate the importance of turbulence model selection for combustor simulation, we simulated methane combustion in a 3D concentric mixer combustor geometry using *OpenFOAM* with simplified single reaction kinetics: $CH_4 + 2O_2 \rightarrow CO_2 + 2H_2O$. Fig. 7 shows the temperature fields calculated from two linear models and a quadratic model for the same configuration, including the same combustion model. All three models exhibit qualitatively different results. Turbulence model selection therefore plays a key role, motivating the generation of turbulence models specific to the flow physics characteristic of sCO_2 for combustion simulation. Chen et al. [2] tabulate the parameters of 12 authors' efforts to perform CFD simulations of oxy-fuel combustion with the vast majority of these authors employing linear k-ε formulations. Establishing turbulence models appropriate for combustion in sCO_2 will therefore add substantial value to the community.

(a) Linear

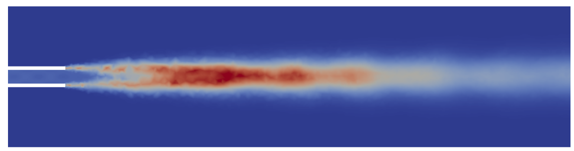

(b) Linear

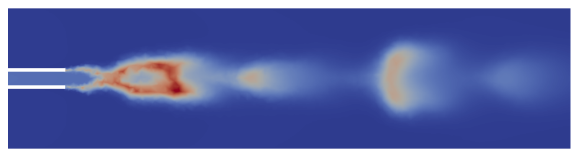

(c) Quadratic

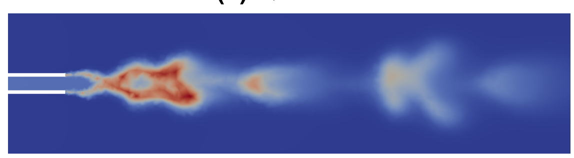

Figure 7: Temperature profiles from a collinear combustor simulation with different turbulence models. Fuel is injected through the small inner cylinder on the left while air in injected through through the larger outer cylinder. The white rectangles are the region separating the two flows before mixing and combustion.

4.1.3 Turbomachinery

Compressors add energy to the fluid causing substantial rise in pressure, which in turn leads to a corresponding increase in density. Turbines remove energy from the fluid leading to lower pressure and density at the outlet. Thus, a proper choice of EOS is critical for both applications. For the anticipated operating conditions, the flow through turbines is expected to be far away from the critical point. At states marginally above the critical point CO_2 compressibility is low, however, and can therefore be pumped more economically. Because of this, many direct-fired Brayton cycles are currently being designed such that the compressor inlet conditions are marginally in the supercritical regime [31].

The primary compressor of a recompression sCO_2 cycle is expected to be of centrifugal type because of the design's capacity to handle large fluid density variations [31]. To lay the groundwork for application to complex simulations, we simulated a simple centrifugal pump with *OpenFOAM*. The pressure gain across the pump is shown in Fig. 8 for a low impeller rotation rate (top) and a high rotation rate (bottom). As is evident from comparing the low and high rotation rates in the figure, the performance of the pump depends substantially on the operating conditions. While turbomachinery models for gases and liquids are quite mature [32], models for supercritical fluids are significantly more nascent. As pumps and turbines are designed for sCO_2 power cycles, accompanying computational models must be incorporated as part of the process. Optimization activities generally require many model evaluations and our future work will entail the development of RANS models specific to turbomachinery for sCO_2 working fluids.

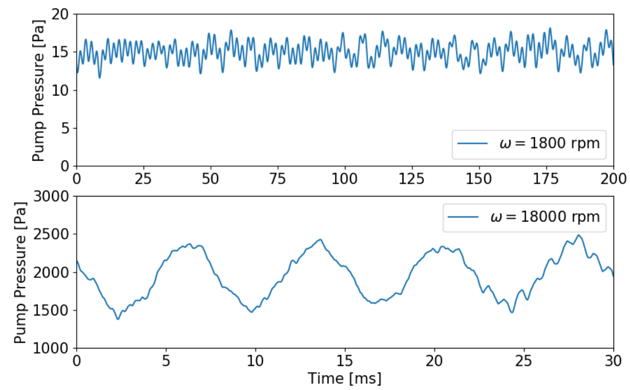

Figure 8: Pressure gain from illustrative centrifugal pump.

Schobeiri and Abdelfattah [33] carried out a combined numerical-experimental study to ascertain the effectiveness of RANS models at modeling high pressure turbines. They noted that secondary flows amount to 40-50% of the pressure loss through a high pressure turbine with a small aspect ratio. RANS models for efficiency optimization must be able to resolve this phenomenon. Future work will involve evaluation of more sophisticated constitutive relations for sCO_2 turbulence.

5 Acknowledgments

This material is based upon work supported by the U.S. Department of Energy, Office of Science, Small Business Innovation Research (SBIR) Program under Award Number(s) Grant No. DE-SC0017236.

References

[1] Roger E. Anderson, Scott MacAdam, Fermin Viteri, Daniel O. Davies, James P. Downs, and Andrew Paliszewski. Adapting gas turbines to zero emission oxy-fuel power plants. *ASME Paper No. GT2008-51377*, 2008.

[2] Lei Chen, Sze Zheng Yong, and Ahmed F. Ghoniem. Oxy-fuel combustion of pulverized coal: Characterization, fundamentals, stabilization and CFD modeling. *Progress in Energy and Combustion Science*, 38(2):156–214, April 2012.

[3] Aaron McClung, Klaus Brun, and Lalit Chordia. Technical and economic evaluation of supercritical oxy-combustion for power generation. In *4th International Supercritical CO2 Power Cycles Symposium*, 2014.

[4] Yoonhan Ahn, Seong Jun Bae, Minseok Kim, Seong Kuk Cho, Seungjoon Baik, Jeong Ik Lee,

and Jae Eun Cha. Review of supercritical CO 2 power cycle technology and current status of research and development. *Nuclear Engineering and Technology*, 47(6):647–661, 2015.

[5] U. S. Department of Energy. Quadrennial Technology Review 2015 Chater 4: Advancing Clean Electric Power Technologies. Technical report, 2015.

[6] Andrea Pucciarelli, Irene Borroni, Medhat Sharabi, and Walter Ambrosini. Results of 4-equation turbulence models in the prediction of heat transfer to supercritical pressure fluids. *Nuclear Engineering and Design*, 281:5–14, 2015.

[7] Ge Zhang, Hao Zhang, Hanyang Gu, Yanhua Yang, and Xu Cheng. Experimental and numerical investigation of turbulent convective heat transfer deterioration of supercritical water in vertical tube. *Nuclear Engineering and Design*, 248:226–237, July 2012.

[8] Y. Nagano and C. Kim. A two-equation model for heat transport in wall turbulent shear flows. *Journal of heat transfer*, 110(3):583–589, 1988.

[9] Romney B. Duffey and Igor L. Pioro. Experimental heat transfer of supercritical carbon dioxide flowing inside channels (survey). *Nuclear Engineering and Design*, 235(8):913–924, 2005.

[10] Joong Hun Bae, Jung Yul Yoo, and Haecheon Choi. Direct numerical simulation of turbulent supercritical flows with heat transfer. *Physics of fluids*, 17(10):105104, 2005.

[11] Keke Xu, Bo Ruan, and Hua Meng. Validation and analyses of RANS CFD models for turbulent heat transfer of hydrocarbon fuels at supercritical pressures. *International Journal of Thermal Sciences*, 124:212–226, 2018.

[12] K. Abe, T. Kondoh, and Y. Nagano. A new turbulence model for predicting fluid flow and heat transfer in separating and reattaching flowsI. Flow field calculations. *International journal of heat and mass transfer*, 37(1):139–151, 1994.

[13] K. Abe, T. Kondoh, and Y. Nagano. A new turbulence model for predicting fluid flow and heat transfer in separating and reattaching flowsII. Thermal field calculations. *International Journal of Heat and Mass Transfer*, 38(8):1467–1481, 1995.

[14] C. B. Hwang and C. A. Lin. A low Reynolds number two-equation k$eta$$eta$ model to predict thermal fields. *International journal of heat and mass transfer*, 42(17):3217–3230, 1999.

[15] Baoqing Deng, Wenquan Wu, and Shitong Xi. A near-wall two-equation heat transfer model for wall turbulent flows. *International journal of heat and mass transfer*, 44(4):691–698, 2001.

[16] S. Kenjereš, S. B. Gunarjo, and K. Hanjalić. Contribution to elliptic relaxation modelling of turbulent natural and mixed convection. *International Journal of Heat and Fluid Flow*, 26(4):569–586, 2005.

[17] Yoon-Yeong Bae, Eung-Seon Kim, and Minhwan Kim. Assessment of low-Reynolds number k- turbulence models against highly buoyant flows. *International Journal of Heat and Mass Transfer*, 108:529–536, 2017.

[18] Yoon-Yeong Bae, Eung-Seon Kim, and Minhwan Kim. Numerical simulation of upward flowing supercritical fluids using buoyancy-influence-reflected turbulence model. *Nuclear Engineering and Design*, 324:231–249, 2017.

[19] F. Ries, P. Obando, I. Shevchuck, J. Janicka, and A. Sadiki. Numerical analysis of turbulent flow dynamics and heat transport in a round jet at supercritical conditions. *International Journal of Heat and Fluid Flow*, 66:172–184, 2017.

[20] Dong Eok Kim and Moo-Hwan Kim. Experimental investigation of heat transfer in vertical upward and downward supercritical CO2 flow in a circular tube. *International Journal of Heat and Fluid Flow*, 32(1):176–191, 2011.

[21] Florian R. Menter. Two-equation eddy-viscosity turbulence models for engineering applications. *AIAA journal*, 32(8):1598–1605, 1994.

[22] Florian Menter and Thomas Esch. Elements of industrial heat transfer predictions. In *16th Brazilian Congress of Mechanical Engineering (COBEM)*, volume 109, 2001.

[23] Florian R. Menter, Martin Kuntz, and Robin Langtry. Ten years of industrial experience with the SST turbulence model. *Turbulence, heat and mass transfer*, 4(1):625–632, 2003.

[24] Antti Hellsten. Some improvements in Menter's k-omega SST turbulence model. In *29th AIAA, Fluid Dynamics Conference*, page 2554, 1998.

[25] W. Xu, Q. Chen, and F. T. M. Nieuwstadt. A new turbulence model for near-wall natural convection. *International Journal of Heat and Mass Transfer*, 41(21):3161–3176, 1998.

[26] T. J. Craft, S. E. Gant, A. V. Gerasimov, Hector Iacovides, and B. E. Launder. Development and application of wall-function treatments for turbulent forced and mixed convection flows. *Fluid Dynamics Research*, 38(2):127–144, 2006.

[27] P. Kiš and H. Herwig. The near wall physics and wall functions for turbulent natural convection. *International Journal of Heat and Mass Transfer*, 55(9):2625–2635, 2012.

[28] Giorgio Soave. Equilibrium constants from a modified Redlich-Kwong equation of state. *Chemical Engineering Science*, 27(6):1197–1203, 1972.

[29] K. R. V. Manikantachari, Scott Martin, Jose O. Bobren-Diaz, and Subith Vasu. Thermal and Transport Properties for the Simulation of Direct-Fired sCO2 Combustor. *Journal of Engineering for Gas Turbines and Power*, 139(12):121505, 2017.

[30] Pallab Ghosh. Prediction of Vapor-Liquid Equilibria Using Peng-Robinson and Soave-Redlich-Kwong Equations of State. *Chemical engineering & technology*, 22(5):379–399, 1999.

[31] Nathan Weiland and David Thimsen. A practical look at assumptions and constraints for steady state modeling of sCO2 Brayton power cycles. In *The 5th International SymposiumSupercritical CO2 Power Cycles*. San Antonio Texas, 2016.

[32] James Tyacke, Paul Tucker, Richard Jefferson-Loveday, Nagabushana Rao Vadlamani, Robert Watson, Iftekhar Naqavi, and Xiaoyu Yang. Large eddy simulation for turbines: methodologies, cost and future outlooks. *Journal of Turbomachinery*, 136(6):061009, 2014.

[33] M. T. Schobeiri and S. Abdelfattah. On the reliability of RANS and URANS numerical results for high-pressure turbine simulations: a benchmark experimental and numerical study on performance and interstage flow behavior of high-pressure turbines at design and off-design conditions using two different turbine designs. *Journal of Turbomachinery*, 135(6):061012, 2013.